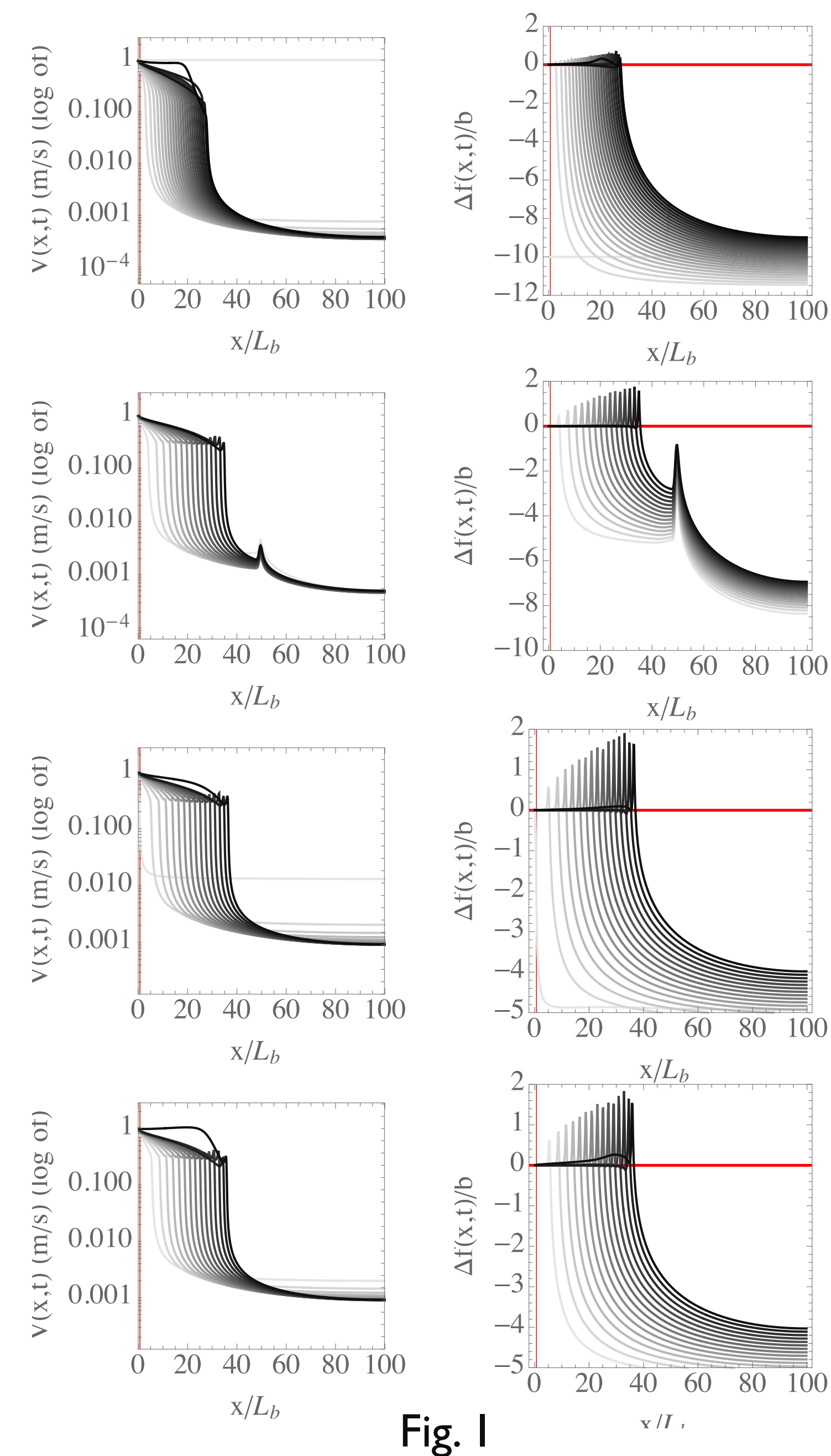


## 2. Dislocation driven semi-infinite fault with with free end



**Large faults:** we find that initially locked faults exhibit a stable creep propagation over long distances along the fault before nucleating an instability in slip velocity. The creep run-out distances, before nucleating an instability, are considerably larger than the elasto-frictional nucleation length-scales inferred by linear stability analyses of steady-sliding and predicted by nonlinear analysis of slip instabilities. After nucleation of the first dynamic rupture, the subsequent aseismic creep run-out distances are larger than the first creep event (Fig. 1). The aseismic slip propagation, driven by a tectonic dislocation at one end, remains unaffected by conditions at the other end for large faults. Fig. 2 indicates how the creep propagation distance varies with initially  $\Delta f_{in}$  for large faults.

Creep penetration for:  $L_{fault}/L_b=50$  and 100

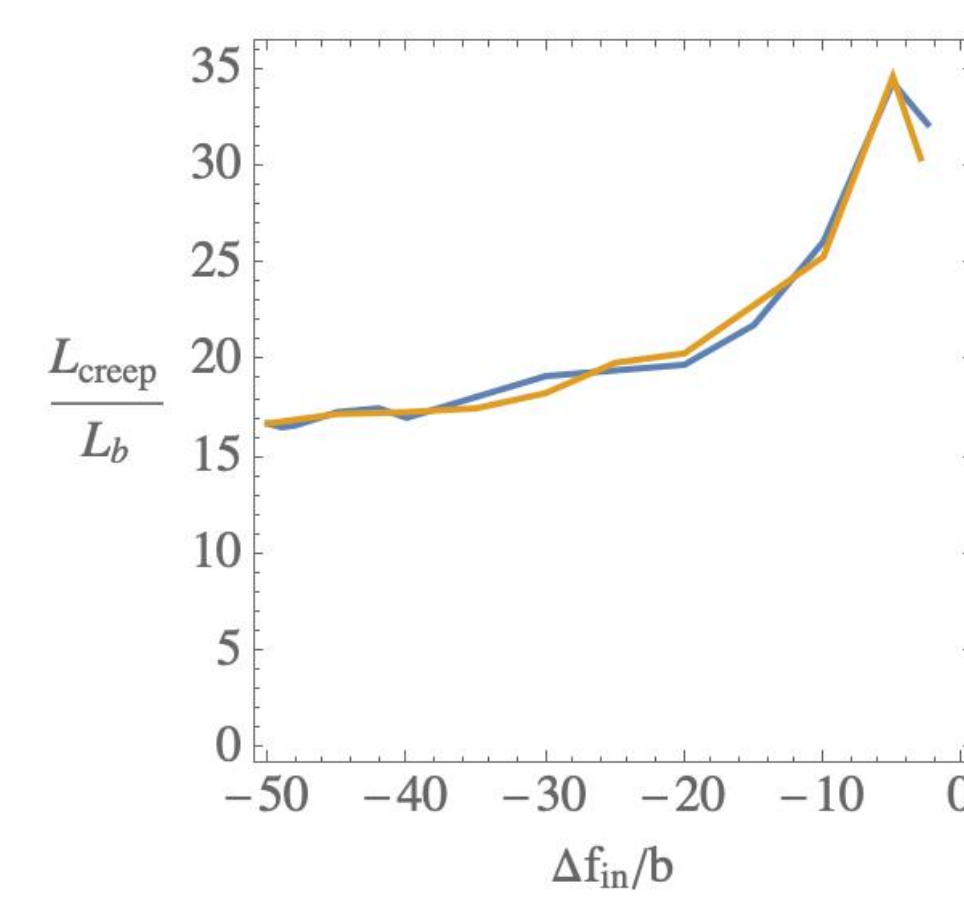


Fig. 2

## 3a. Finite fault with the other end buried/locked

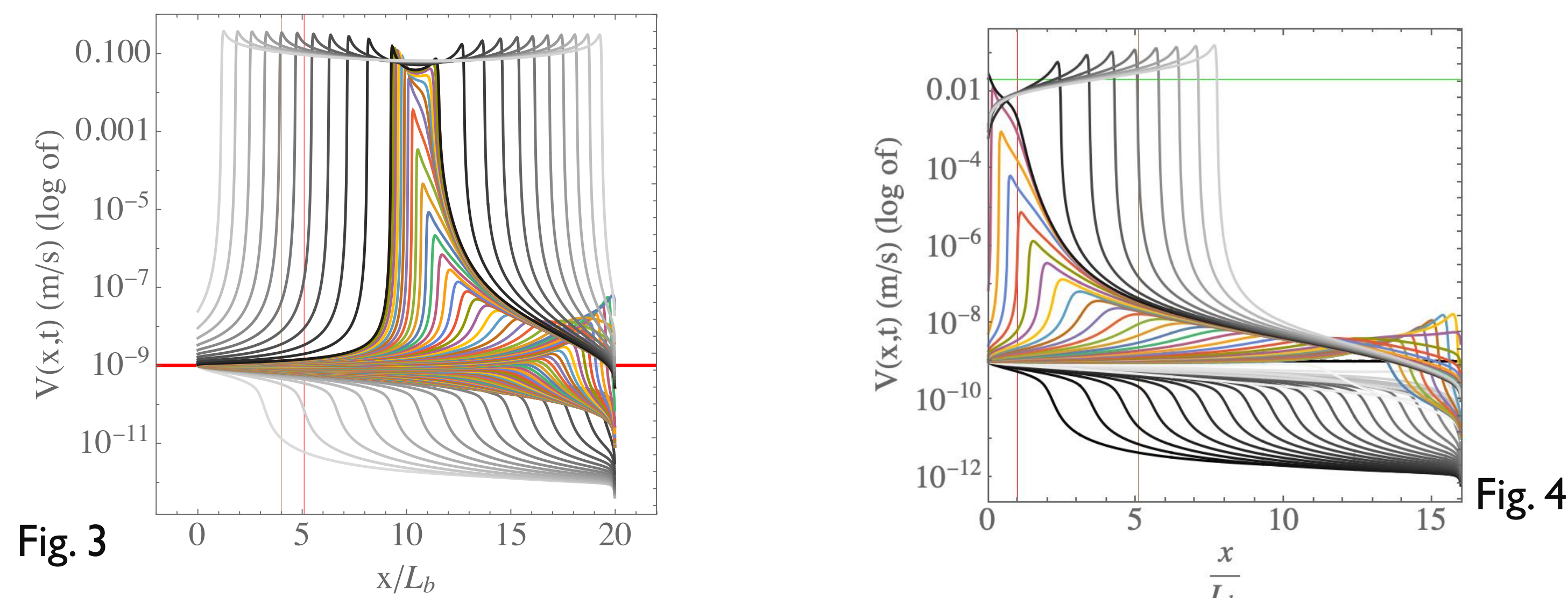


Fig. 3

A strictly locked end has interesting consequences on dislocation-driven creep advance. In this case, the slow aseismic creep provokes instability only when the finite-fault size exceeds a cut-off size,  $L_c$ . Further, on such finite-faults of size larger than standard nucleation length-scales but lesser than the cut-off size,  $L_c$ , a propagating creep could fail to nucleate an instability, and instead, could continue to lock or exhibit a long sustained spatio-temporal type oscillation, breathing type evolution of slip rate.

## 3b. A breathing type slip-rate evolution

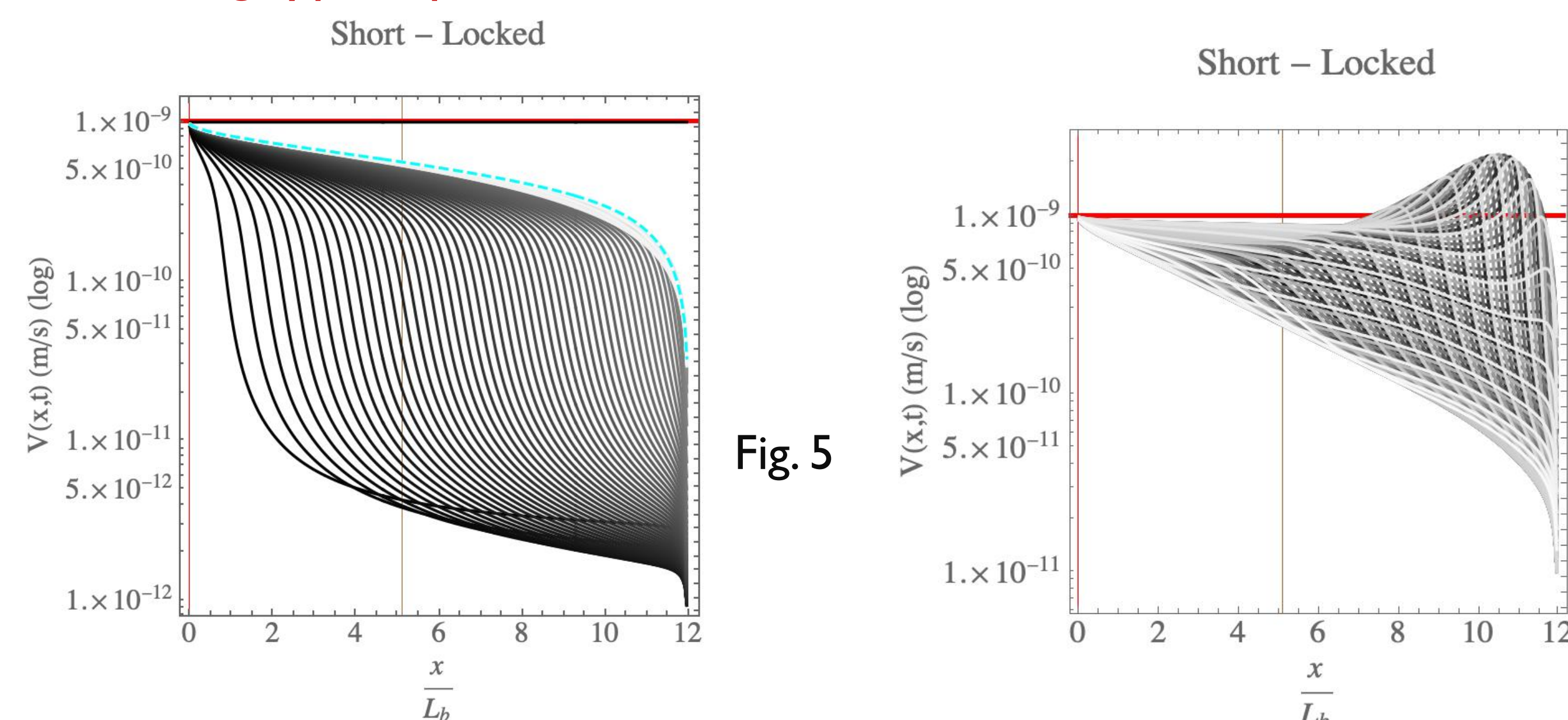


Fig. 5

## I. Introduction

We highlight how slow aseismic slip travels long distances on rate-weakening interfaces. We considered model faults with sliding rate- and state-dependent interfacial shear strength. The slip is driven by a tectonic dislocation (accrued at a constant rate at one end) on a finite fault with the other end either locked or free. We also consider scenarios where slip is driven by dislocations imposed at both the ends or spatially localized external stress.

### Shear stress and its rate on the fault

$$\tau(x, t) = \tau_b(x, t) + \tau_{el}[\delta(x, t), t] - \frac{\mu'}{2c_s} V(x, t)$$

$$\frac{\partial \tau}{\partial t} = \frac{\partial \tau_b}{\partial t} + \frac{\partial \tau_{el}}{\partial t} - \frac{\mu'}{2c_s} \frac{\partial V}{\partial t}$$

### Medium's (elastic) response to slip

$$\tau_{el}[\delta(x, t), t] = \frac{\mu'}{2\pi} \int_{-L/2}^{L/2} \frac{\partial \delta(x', t)/\partial x'}{x' - x} dx'$$

### Shear strength under constant normal stress = 0

$$\tau_s(x, t) = \sigma f(V, \Theta) \quad \frac{\partial \tau_s}{\partial t} = \sigma \frac{\partial f}{\partial t}$$

### Friction Coefficient

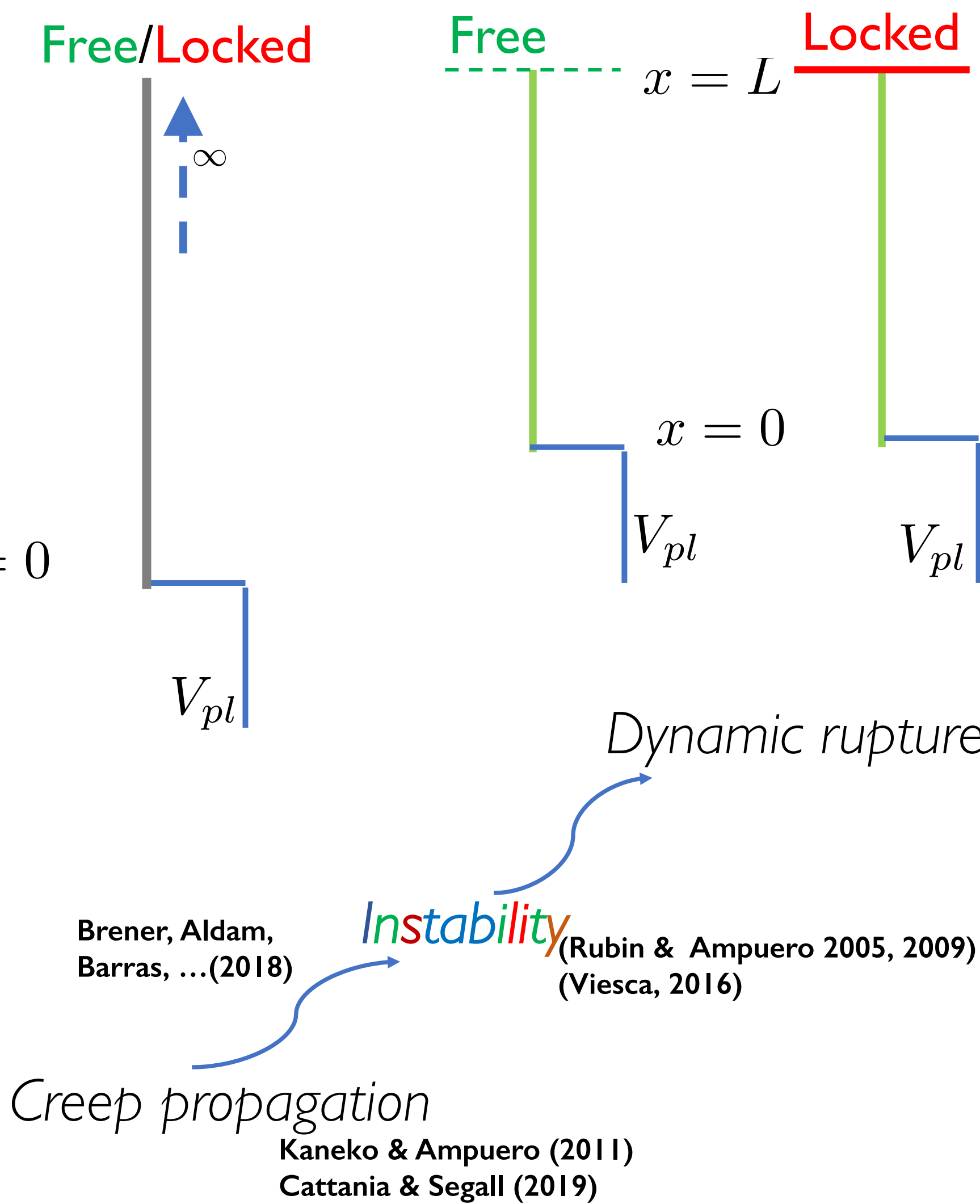
$$f(V, \theta) = f_o + a \ln \left( \frac{V(x, t)}{V_o} \right) + \Theta(x, t)$$

### Steady state behavior

$$f(V) = f_o + (a - b) \ln \left( \frac{V(x, t)}{V_o} \right)$$

### Deviation from steady-state sliding

$$\Delta f(x, t) = f(V, \Theta) - f(V)$$



## 4 Finite faults with the other end free

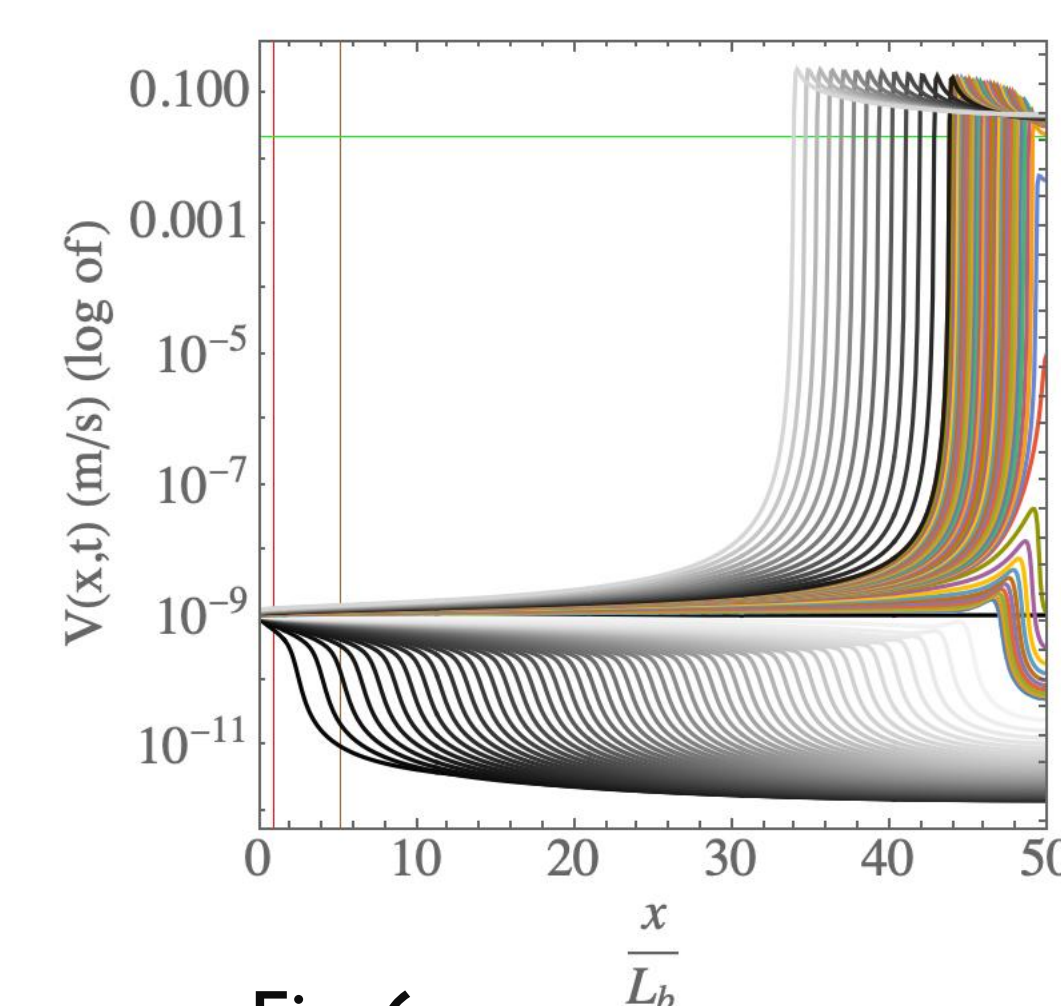


Fig. 6

A finite fault driven by dislocations at both the ends (or a finite-fault with free-surface at the other end), transition to instability does not involve such breathing type oscillation of slip rate.

## 5. Dislocations drive slip from two ends

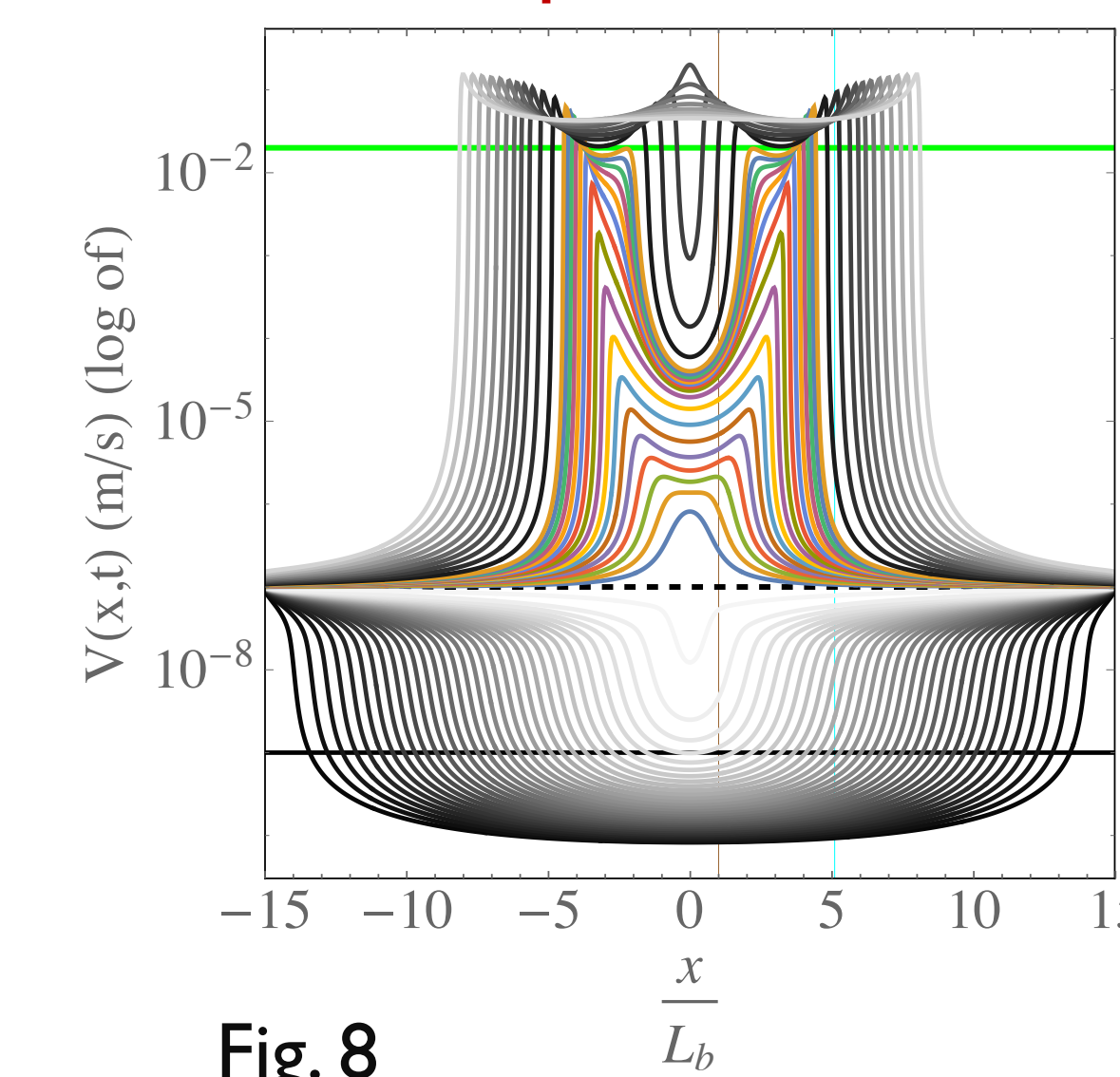


Fig. 8

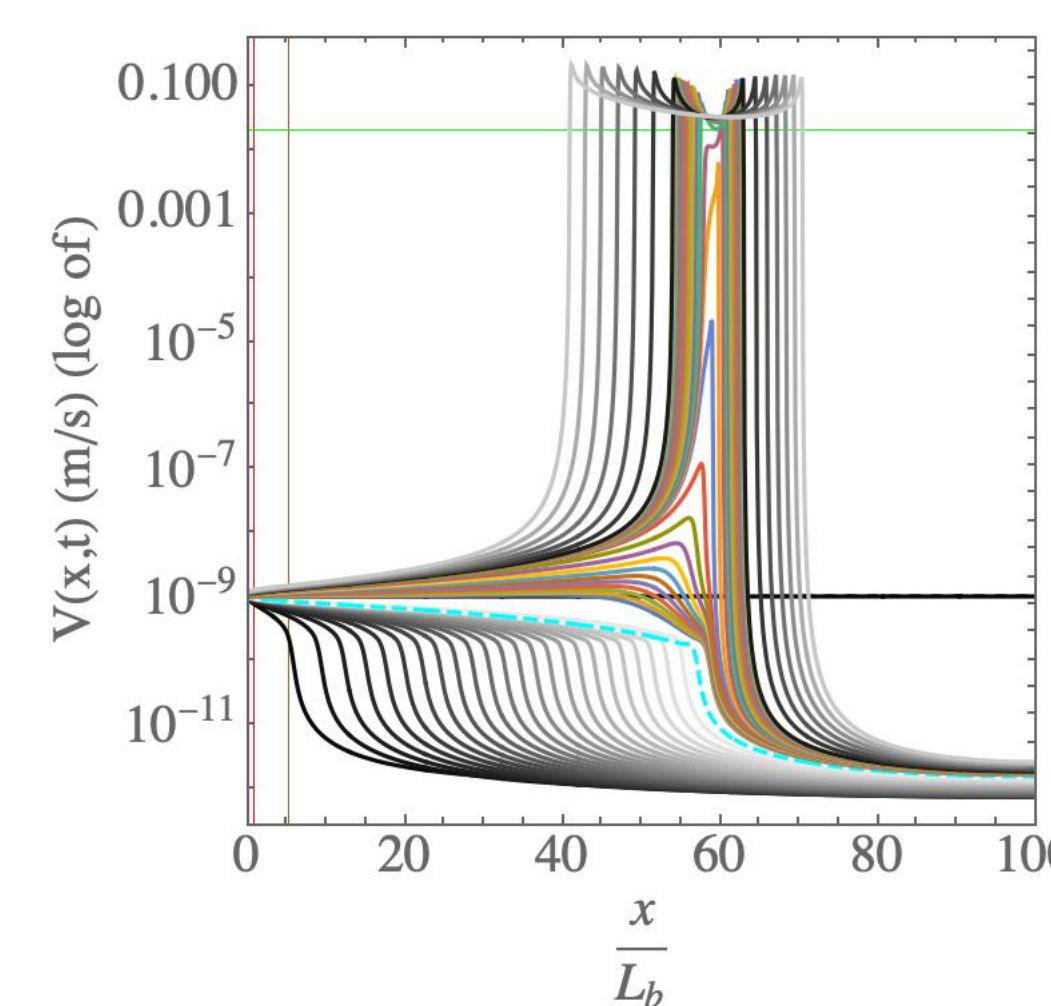


Fig. 7

Large faults with the other end free

## 6. Equivalent crack model for the creep propagation

Here we consider a long (semi-infinite) fault where the slip is driven by an imposed dislocation at the one end. We look for the elastodynamic stress transfers in a coordinate  $\zeta = v_r t - x$  that moves with the tip of the rupturing front.

$$\tau[\delta(\zeta)] = \tau_{ex} + \frac{\mu' \sqrt{1 - v_r^2/c^2}}{2\pi} \int_0^\infty \frac{\delta'(\tilde{\zeta})}{\tilde{\zeta} - \zeta} d\tilde{\zeta} \quad \text{where}$$

$v_r$  is the rupture speed.

Following Garagash (Phil. Trans. Roy. Soc., 2020), we consider an equivalent crack that slips under imposed dislocation and an effective stress drop,  $\Delta \tau_{eff}$ , from background stress to steady-state sliding at an effective slip rate. When slip occurs, we have

$$F(l, v_r, t) \equiv \frac{V_{dis} \cdot t}{\pi l(t)} + \frac{\Delta \tau_{eff}}{\mu'} - \frac{K_c}{\mu' \sqrt{\pi l/2}} = 0$$

where the toughness is determined from friction conditions and rupture speed., given by

$$K_c = \frac{E(1 - v_r^2/c^2)}{(1 - v_r^2/c^2)^{1/4}} \sqrt{2\mu G_c} \quad \text{where} \quad G_c = \frac{\Delta f_p}{b} (b\bar{\sigma} D_c)$$

We obtained slip rate of the equivalent crack, given by

$$V = \frac{1}{P} \left[ \sqrt{\frac{\xi}{1 - \xi}} + \frac{2}{\pi} \mathcal{P} \sin^{-1} \left( \sqrt{1 - \xi} \right) \right] \quad \text{where} \quad P = \frac{K_c v_r}{\mu' \sqrt{\pi l/2}}$$

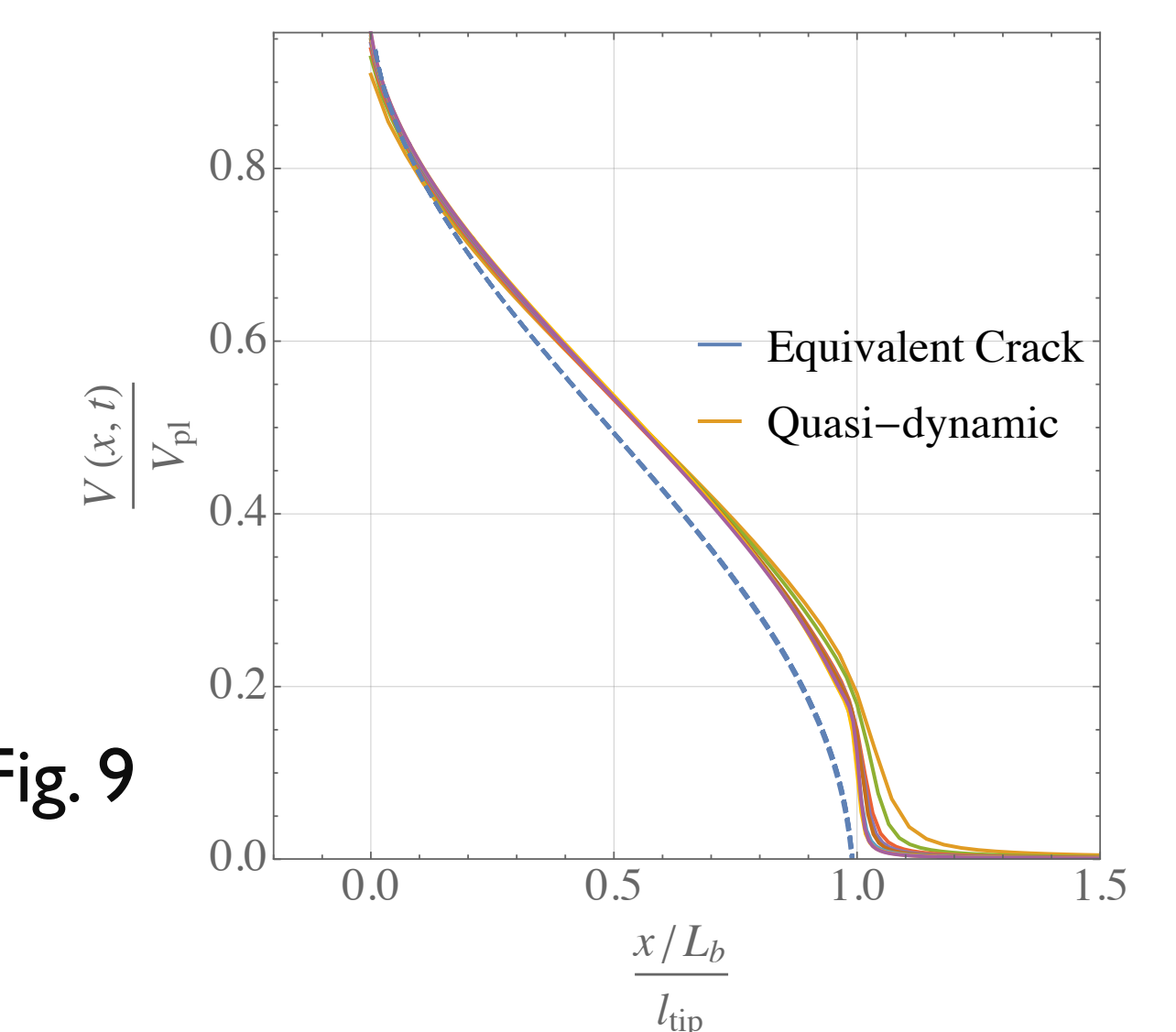


Fig. 9

## 7. Notations

effective normal stress: $\sigma$	Fracture energy: $G_c$
shear traction: $\tau$	Fracture toughness: $K_c$
shear strength: $\tau_s$	Stress Intensity Factor: $K$
friction coefficient: $f$	Rupture length: $l$
State Variable: $\Theta$	Peak Friction departure: $\Delta f_p$
Direct effect: $a$	Friction evolution slip scale: $D_c$
Evolution effect: $b$	Elliptic Integral IInd kind: $E$
Away from steady-state sliding: $\Delta f$	
slip rate: $V$	
rupture speed: $v_r$	
wave speed: $c$	
coordinate: $\zeta, x$	

## 8. References

1. Rubin and Ampuero (JGR, 2009)
2. Kaneko and Ampuero (JGR, 2011)
3. Brener et al. (2018)
4. Bar-Sinai et. al. (2019)
5. Cattania and Segall (JGR, 2019)
6. Garagash (PTRS, 2020)